



International Journal of Powertrains

ISSN online: 1742-4275 - ISSN print: 1742-4267

<https://www.inderscience.com/ijpt>

Energy management of hybrid electric vehicle based on linear time-varying model predictive control

Daofei Li, Jiajie Zhang, Dongdong Jiang

DOI: [10.1504/IJPT.2024.10063524](https://doi.org/10.1504/IJPT.2024.10063524)

Article History:

Received:	11 January 2022
Last revised:	30 March 2023
Accepted:	18 May 2023
Published online:	16 April 2024

Energy management of hybrid electric vehicle based on linear time-varying model predictive control

Daofei Li*, Jiajie Zhang and Dongdong Jiang

Institute of Power Machinery and Vehicular Engineering,

College of Energy Engineering,

Zhejiang University, China

Email: dfli@zju.edu.cn

Email: 3180104720@zju.edu.cn

Email: jiangdongdong@zju.edu.cn

*Corresponding author

Abstract: Energy management of hybrid electric vehicle (HEV) is crucial for improving fuel economy and reducing emissions. Due to the challenges in both development and implementation, simplified algorithms using rule-based strategies or equivalent consumption minimisation strategy (ECMS), still prevail in real vehicle applications. Taking an HEV with P2 hybrid powertrain for example, a bi-level hybrid model predictive control (bi-HMPC) algorithm is proposed. The upper level calculates the optimal engine/motor torque distribution based on linear time-varying model predictive control (LTV-MPC), while the lower level optimises the gear ratio via hybrid model predictive control (HMPC). The algorithm is preliminarily validated via simulations, which demonstrate that it has better fuel-saving performances than ECMS. Then the LTV-MPC is implemented in real vehicle and validated via dynamometer tests. Results show that it can run real-time and reduce the fuel consumption from 7.05 L/100 km to 6.2 L/100 km, together with noticeable improvements in pollutant emissions.

Keywords: hybrid electric vehicle; HEV; energy management; linear time varying model predictive control; fuel economy; real vehicle tests.

Reference to this paper should be made as follows: Li, D., Zhang, J. and Jiang, D. (2024) 'Energy management of hybrid electric vehicle based on linear time-varying model predictive control', *Int. J. Powertrains*, Vol. 13, No. 1, pp.95–111.

Biographical notes: Daofei Li received his BS in Vehicle Engineering from the Jilin University, Changchun, China, in 2003, and his PhD in Vehicle Engineering from the Shanghai Jiao Tong University, Shanghai, China, in 2008. Since June 2008, he joined the Institute for Power Machinery and Vehicular Engineering, Faculty of Engineering, Zhejiang University (ZJU), Hangzhou, China. He was a Visiting Scholar with the University of Missouri-Columbia in 2011, and later with the University of Michigan, Ann Arbor, Michigan from 2014 to 2016. He is currently an Associate Professor with ZJU and directs the Research Group of Human-Mobility-Automation. His research interests include vehicle dynamics and control, driver model, and autonomous driving.

Jiajie Zhang received his BS of Vehicle Engineering from the Zhejiang University, Hangzhou, China, in 2022. He joined the Research Group of Human-Mobility-Automation, ZJU in August 2021 and is currently pursuing for his MS of Power Engineering. His research interests include eco-driving, vehicle dynamic control, motion planning, and driver model.

Dongdong Jiang received his BS in Mechanical Design, Manufacturing and Automation (Automotive Engineering) from the Zhejiang University, Hangzhou, China, in 2012, and his PhD in Power Machinery and Engineering from the Zhejiang University, Hangzhou, China, in 2020. During his PhD study, his research interests included vehicle control, energy management for hybrid vehicles, and connected and automated vehicles. He is currently with Li Auto Inc.

This paper is a revised and expanded version of a paper entitled ‘Energy management of hybrid electric vehicle based on linear time-varying model predictive control’ presented at International Conference on Advanced Vehicle Powertrains, Beijing, China, 2–4 September 2021.

1 Introduction

To cope with energy shortages and environmental pollution, the automakers have proposed various of new energy vehicle strategies. Hybrid electric vehicle (HEV) is one of the promising short-term solutions (Bayindir et al., 2011). In HEV, internal combustion engine (ICE) can work more efficiently, based on the working point coordination with electric motor/generators (Liu and Peng, 2008). According to a recent report by Mordor Intelligence (2021), the global HEV market is expected to reach a value of USD1,166.65 billion by 2026, registering a compound annual growth rate of 29.13% from 2021 to 2026. In China, under the pressure of the so-called dual credit policy, including corporate average fuel consumption and new energy vehicle credit regulation, the automakers are pushing for both pure and HEVs.

As the core technology of HEV development, energy management is to coordinate the engine and motors/generators for optimised fuel economy and pollutant emission, while guaranteeing responsive power performance required by driver or upper level controls. Rule-based approaches are still popular in real applications, but their developments, including rule setting and parameter calibrations, are usually time-consuming. The optimisation-based solutions are getting more and more attention from algorithm developers. This is made possible due to their excellent capabilities in capturing the entire problems from system modelling to control solutions, including the handling of multiple objectives and constraints.

However, the optimal energy management problem is basically a nonlinear, constrained, and dynamic optimisation problem due to the nonlinearities of certain dynamic powertrain model (Borhan et al., 2010). Dynamic programming (DP) (Lin et al., 2004) or equivalent consumption minimisation strategy (ECMS) (Serrao et al., 2009) are well-studied in the past decades. Pisu et al. gave a detailed derivation of equivalent

conversion coefficient in ECMS (Pisu and Rizzoni, 2005; Pisu et al., 2005). Musardo et al. (2005) proposed a new adaptive ECMS and realised real-time energy management of HEV. On the other hand, model predictive control (MPC) is also an algorithm widely studied and used in industrial applications (Cairano et al., 2007; Lee, 2011), though usually MPC has disadvantages of computing load and difficult handling with nonlinear HEV models. To cope with this challenge, Iyama and Namerikawa (2014) made the linearisation of the nonlinear model by constantly switching the corresponding model parameters. Borhan et al. (2011) also tried to linearise the model and applied linear time-varying model predictive control (LTV-MPC). However, there are still limited reports on its implementation for HEV energy management in real vehicles. On the other hand, Jiang et al. (2020a) attempted to optimise HEV's torque distribution and gear ratio simultaneously via a complicated hybrid model predictive control (HMPC), which has difficulty in real-time calculation due to model's complexity.

In this paper, we develop a bi-level optimisation algorithm for the energy management of a P2 hybrid passenger vehicle and carry out several simulations to validate the proposed algorithm. The upper LTV-MPC-based torque optimisation is further validated in real-vehicle experiments. The contribution of this paper is as follows.

- 1 A bi-level algorithm for energy management of a P2 hybrid passenger vehicle is proposed. The original hybrid nonlinear optimisation problem is divided into two sub-problems, i.e., the engine/motor torque distribution optimisation is solved using linear time varying MPC in the upper level and then transmission ratio optimisation is realised in the lower level.
- 2 Both simulation and bench tests are carried out, showing the proposed algorithm can run in real-time and realise effective implementation in a real vehicle. With only three rounds of bench tests, the model-based controller can achieve promising fuel consumption performances close to the original rule-based strategy (RB), which in contrast is time-consuming in development and testing. The proposed controller shows great potential in accelerating the controller development in real practice.

The rest of this paper is organised as follows. Section 2 introduces our HEV system model. In Section 3, we formulate the energy management strategy based on a linear time-varying MPC. Then simulation results are presented in Section 4 and a series of real vehicle test results are shown in Section 5, which prove our LTV-MPC's ability in improving fuel economy. Finally, conclusions are given in Section 6.

2 Vehicle modelling

A P2 hybrid passenger vehicle, as schemed in Figure 1, is taken as the target vehicle for the development of energy management strategy. By adding an electric motor and a disconnecting clutch between the engine and transmission in a traditional ICE vehicle, the electric motor can work in either driving or generating modes. Table 1 lists the basic HEV parameters. The bench test data of its engine and motor are presented in Figure 2, i.e., brake specific fuel consumption (BSFC) for engine and overall efficiency for motor, respectively.

Figure 1 Block diagram of P2 type HEV (see online version for colours)

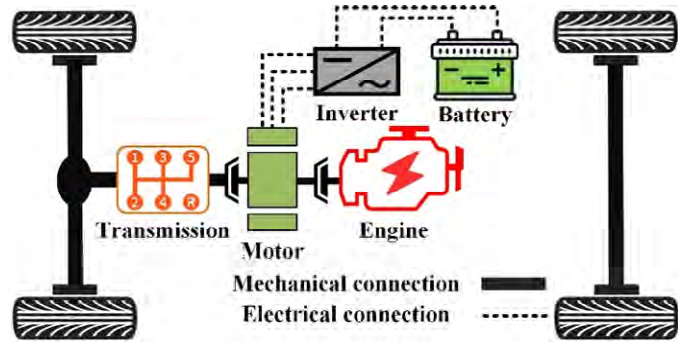
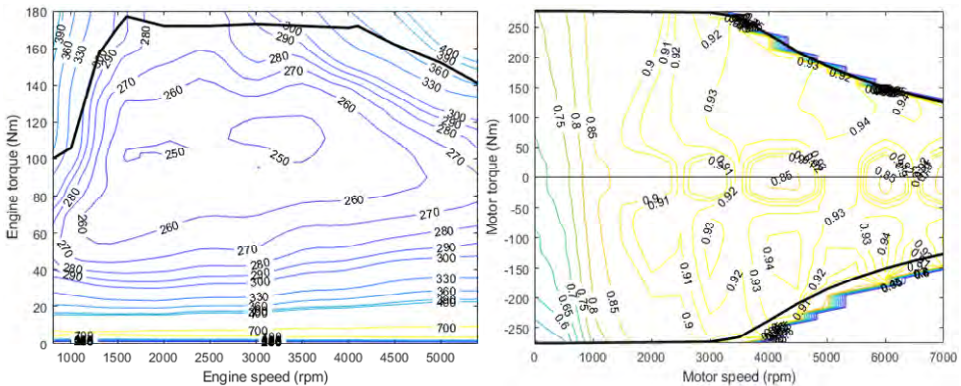


Table 1 Basic parameters of the studied HEV

Parameters	Value	Parameters	Value
Mass	1,600 (kg)	Final reduction ratio	2.808
Tire radius	0.32 (m)	Mechanical efficiency of drivetrain	0.95
Vehicle frontal area	2.275 (m ²)	Battery internal resistance	0.1 (Ω)
Transmission gear ratios	I:5.22; II:3.11; III:2.13; IV:1.57; V:1.27; VI:1.05; VII:0.89	Battery capacity	11 (kWh)/30 (Ah@370V)
Engine's maximum torque/power	180 (N·m)/86 (kW)	Motor's maximum torque/power	260 (N·m)/80 (kW)

Figure 2 The BSFC data of engine (in g/kWh) and overall efficiency of motor (see online version for colours)



According to Figure 2, the nonlinear models of engine (F) and motor (G) are obtained via polynomial fitting, similarly to that in our previous publication (Jiang et al., 2020b).

$$\begin{aligned}
\dot{m}_f &= F(T_{eng}, \omega_{eng}) \\
&= f_{00} + f_{10}\omega_{eng} + f_{01}T_{eng} + f_{20}\omega_{eng}^2 + f_{11}\omega_{eng}T_{eng} + f_{02}T_{eng}^2 + f_{30}\omega_{eng}^3 \\
&\quad + f_{21}\omega_{eng}^2T_{eng} + f_{12}\omega_{eng}T_{eng}^2 + f_{03}T_{eng}^3 + f_{40}\omega_{eng}^4 + f_{31}\omega_{eng}^3T_{eng} \\
\eta_{mot} &= G(T_{mot}, \omega_{mot}) \\
&= p_{00} + p_{10}\omega_{mot} + p_{01}T_{mot} + p_{20}\omega_{mot}^2 + p_{11}\omega_{mot}T_{mot} + p_{02}T_{mot}^2 + p_{30}\omega_{mot}^3 \\
&\quad + p_{21}\omega_{mot}^2T_{mot} + p_{12}\omega_{mot}T_{mot}^2 + p_{40}\omega_{mot}^4 + p_{31}\omega_{mot}^3T_{mot} + p_{22}\omega_{mot}^2T_{mot}^2 \\
&\quad + p_{50}\omega_{mot}^5 + p_{41}\omega_{mot}^4T_{mot} + p_{32}\omega_{mot}^3T_{mot}^2
\end{aligned} \tag{1}$$

where \dot{m}_f is the fuel consumption rate of engine, T_{eng} and ω_{eng} represent engine torque and speed, respectively. η_{mot} , T_{mot} and ω_{mot} represent motor efficiency, torque and speed, respectively. The model coefficients are listed in Table 2.

Table 2 Coefficients of nonlinear models F and G

Coefficients of F			Coefficients of G		
$f_{00} = 3.9\text{e-}1$	$f_{10} = -2.7\text{e-}3$	$f_{01} = -2.5\text{e-}2$	$P_{00} = 6.8\text{e-}1$	$P_{10} = 2.2\text{e-}3$	$P_{01} = 3.8\text{e-}4$
$f_{20} = 6.9\text{e-}6$	$f_{11} = 2.6\text{e-}4$	$f_{02} = 3.2\text{e-}4$	$P_{20} = -7.2\text{e-}6$	$P_{11} = -3.7\text{e-}6$	$P_{02} = -6.5\text{e-}7$
$f_{30} = 1.6\text{e-}9$	$f_{21} = -3.8\text{e-}7$	$f_{12} = -2.2\text{e-}6$	$P_{30} = 1.0\text{e-}8$	$P_{21} = 1.4\text{e-}8$	$P_{12} = 1.7\text{e-}9$
$f_{03} = -8.5\text{e-}7$	$f_{40} = -6.1\text{e-}12$	$f_{31} = 1.7\text{e-}10$	$P_{40} = -4.8\text{e-}12$	$P_{31} = -2.0\text{e-}11$	$P_{22} = 2.2\text{e-}13$
$f_{22} = 2.4\text{e-}9$	$f_{13} = 5.2\text{e-}9$		$P_{50} = -3.6\text{e-}16$	$P_{41} = 1.0\text{e-}14$	$P_{32} = -1.8\text{e-}15$

As for battery modelling, this paper uses an equivalent circuit model by referring to Pang et al. (2001). According to Kirchhoff's voltage law and equivalent circuit principle, the formula of current I can be derived as equation (2).

$$I = \frac{V_{oc} - \sqrt{V_{oc}^2 - 4R_{int}P_{batt}}}{2R_{int}} \tag{2}$$

where V_{oc} is open-circuit voltage of battery, and R_{int} and P_{batt} represent internal resistance and power, respectively. The state of charge (SOC) of battery can be obtained via the calculation of total charge/discharge current according to the Coulomb efficiency, i.e.,

$$SOC = \frac{Q_0 - \int Idt}{Q_{batt}} \tag{3}$$

where Q_0 and Q_{batt} denote initial and total charges of the battery, respectively. Combining equations (2) and (3), the change rate of SOC can be drawn as equation (4), where P_{batt} is the battery power.

$$\begin{cases} \dot{SOC} = \frac{V_{oc} - \sqrt{V_{oc}^2 - 4R_{int}P_{batt}}}{2R_{int}Q_{batt}} \\ P_{batt} = T_{mot}\omega_{mot}\eta_{mot} \cdot \text{sign}(T_{mot}\omega_{mot}) \end{cases} \tag{4}$$

Longitudinal dynamics model is used to obtain the vehicle acceleration under different driving torque inputs. The model can be established according to the force analysis and Newton's second law as

$$M\dot{V} = \frac{(T_{eng} + T_{mot})i_g i_0}{R_w} - F_b - F_r \quad (5)$$

where F_r is the total driving resistance, F_b is the vehicle braking force, M is the vehicle mass, R_w is the rolling radius of tyres, V is the vehicle speed, i_g and i_0 are the ratios of the transmission and final reduction, respectively. Here, the total resistance force is composed of air drag, rolling and gradient resistances, i.e.,

$F_r = \frac{1}{2}C_d \rho A V^2 + \mu g M \cos(\theta) + Mg \sin(\theta)$. C_d denotes air drag coefficient, ρ denotes air density, and μ and θ represent road friction coefficient and slope angle of the road, respectively.

3 Bi-level controller development

To propose energy management strategy for the P2 HEV, this paper adopts MPC to optimise the gear ratio and torque distribution of engine and motor. However, the optimisation problem is hybrid since the dual clutch transmission ratios are discrete but not continuous. To address this hybrid problem, a bi-level hybrid model predictive control (bi-HMPC) is developed. The upper level optimises the torque distribution via LTV-MPC, while the lower level formulates the gear ratio optimisation as a HMPC and then solves it through mixed integer quadratic programming (MIQP).

3.1 Torque optimisation based on LTV-MPC

Combining the above model equations (1)–(5), a nonlinear model of HEV can be obtained.

$$\begin{cases} \dot{x} = f(x, u, d) \\ y = g(x, u, d) \end{cases} \quad (6)$$

where the state variable $x = [V, SOC, m_f]^T$, continuous control variable $u = [T_{eng}, T_{mot}]^T$, the disturbance $d = [F_r]$, and the system output $y = [V, SOC, m_f]^T$.

Taylor expansion is employed to linearise the model at the current operating point (x_0, u_0, d_0) of the controlled system, as shown in equation (7). As the operating point moves, system matrices of the linear model will also change.

$$\dot{x} = f(x_0, u_0, d_0) + A(t)(x - x_0) + B_u(t)(u - u_0) + B_d(t)(d - d_0) \quad (7)$$

where

$$A = \left. \frac{\partial f}{\partial x^T} \right|_{(u_0, x_0, d_0)}, B_u = \left. \frac{\partial f}{\partial u^T} \right|_{(u_0, x_0, d_0)}, B_d = \left. \frac{\partial f}{\partial d^T} \right|_{(u_0, x_0, d_0)}.$$

Then we have the continuous state space equation as $\dot{\tilde{x}} = A(t)\tilde{x} + B_u(t)\tilde{u} + B_d(t)\tilde{d}$, where $\tilde{x} = x - x_0$, $\tilde{u} = u - u_0$, $\tilde{d} = d - d_0$. It needs to be discretised for real-time controller as follows,

$$\begin{aligned}\tilde{x}(k+1) &= A(k, t)\tilde{x}(k) + B_u(k, t)\tilde{u}(k) + B_d(k, t)\tilde{d}(k) \\ y(k) &= c(k, t)\tilde{x}(k)\end{aligned}\quad (8)$$

where $A(k, t) = I + dTA(t)\tilde{x}(k)$, $B_u(k, t) = TB_u(t)$, $B_d(k, t) = TB_d(t)$, and dT represents the discretisation step size.

Using the control increment $\Delta u(k)$, we can rewrite the system equation as

$$\zeta(k+1) = \tilde{A}\zeta(k) + \tilde{B}_u\Delta u(k) + \tilde{B}_d\tilde{d}(k), \eta(k) = \tilde{C}\zeta(k) \quad (9)$$

where $\zeta(k) = \begin{bmatrix} \tilde{x}(k) \\ \tilde{u}(k-1) \end{bmatrix}$, $\tilde{A} = \begin{bmatrix} A(k, t) & B_u(k, t) \\ 0 & I \end{bmatrix}$, $\tilde{B}_u = \begin{bmatrix} B_u(k, t) \\ I \end{bmatrix}$, $\tilde{B}_d = \begin{bmatrix} B_d(k, t) \\ 0 \end{bmatrix}$, $\tilde{C} = [C(k, t) 0]$. Then the output of $\tilde{C}\zeta(k)$ is $y(k)$, which contains V , SOC and m_f at step k .

For the MPC design, the prediction horizon is set N_p , the control horizon is N_c . We set $\Delta u(k+i) = 0$, for $i \in [N_c + 1, \dots, N_p]$. Taking the state variable $\zeta(k)$ at k as the initial condition, the state in the prediction horizon can be obtained as equation (10).

$$Y = \psi\zeta(k) + \Theta\Delta U + \Xi D \quad (10)$$

$$\begin{aligned}\text{where } Y &= \begin{bmatrix} \eta(k+1) \\ \eta(k+2) \\ \eta(k+3) \\ \dots \\ \eta(k+N_p) \end{bmatrix}, \psi = \begin{bmatrix} \tilde{C}\tilde{A} \\ \tilde{C}\tilde{A}^2 \\ \dots \\ \tilde{C}\tilde{A}^{N_c} \\ \dots \\ \tilde{C}\tilde{A}^{N_p} \end{bmatrix}, \Xi = \begin{bmatrix} \tilde{C}\tilde{B}_d & 0 & \dots & 0 \\ \tilde{C}\tilde{A}\tilde{B}_d & \tilde{C}\tilde{B}_d & \dots & 0 \\ \vdots & \vdots & \ddots & \vdots \\ \tilde{C}\tilde{A}^{N_p-1}\tilde{B}_d & \tilde{C}\tilde{A}^{N_p-2}\tilde{B}_d & \dots & \tilde{C}\tilde{A}^{N_p-1}\tilde{B}_d \end{bmatrix}, \\ \Theta &= \begin{bmatrix} \tilde{C}\tilde{B}_u & 0 & 0 & 0 \\ \tilde{C}\tilde{A}\tilde{B}_u & \tilde{C}\tilde{B}_u & 0 & 0 \\ \vdots & \vdots & \ddots & \vdots \\ \tilde{C}\tilde{A}^{N_c-1}\tilde{B}_u & \tilde{C}\tilde{A}^{N_c-2}\tilde{B}_u & \dots & \tilde{C}\tilde{B}_u \\ \tilde{C}\tilde{A}^{N_c}\tilde{B}_u & \tilde{C}\tilde{A}^{N_c-1}\tilde{B}_u & \dots & \tilde{C}\tilde{A}\tilde{B}_u \\ \vdots & \vdots & \ddots & \vdots \\ \tilde{C}\tilde{A}^{N_p-1}\tilde{B}_u & \tilde{C}\tilde{A}^{N_p-2}\tilde{B}_u & \dots & \tilde{C}\tilde{A}^{N_p-N_c-1}\tilde{B}_u \end{bmatrix}, \Delta U = \begin{bmatrix} \Delta u(k) \\ \Delta u(k+1) \\ \dots \\ \Delta u(k, N_c) \end{bmatrix}, D = \begin{bmatrix} \tilde{d}(k) \\ \tilde{d}(k+1) \\ \dots \\ \tilde{d}(k+N_p) \end{bmatrix}.\end{aligned}$$

To obtain the optimal control, we define the cost function J as shown in equation (11), including the error between the actual output and the reference output value within the prediction horizon, control increment and control magnitude within the control horizon.

$$\begin{aligned}
J &= \sum_{i=1}^{N_p} \|\eta(k+i) - \eta_{ref}(k+i)\|_Q^2 + \sum_{i=1}^{N_c-1} \|\Delta u(k+i)\|_R^2 + \sum_{i=1}^{N_c-1} \|u(k+i)\|_S^2 \\
&= (Y - Y_{ref})^T Q (Y - Y_{ref}) + \Delta U^T R \Delta U + U^T S U
\end{aligned} \tag{11}$$

where Q , R and S are weights of $\eta(k)$, $\Delta u(k)$ and $u(k)$, respectively. Here, the reference output η_{ref} contains reference velocity V_{ref} , initial value of battery SOC and ideal fuel consumption m_{fref} as 0 g/s, i.e., $\eta_{ref} = [V_{ref}, SOC_{ref}, m_{fref}]^T$.

Here, we define the error $\varepsilon \equiv \psi^\zeta(k) + \Xi D - Y_{ref}$. With this, equation (11) can be rewritten as the standard form of quadratic programming shown in equation (12).

$$J = \Delta U^T H \Delta U + 2f \Delta U + \varepsilon^T Q \varepsilon \tag{12}$$

where $H = \Theta^T Q \Theta + R + L^T S L$, and $f = \varepsilon^T Q \Theta + L^T S u(k-1)$.

For the optimisation problem, the following constraints need to be satisfied, including that of control magnitudes and system outputs. Note that more detailed actuator limits and control objectives, e.g., emission, can also be directly included in the LTV-MPC design process. However, due to the system complexities, especially in the distributed controller functions with multiple considerations on fuel economy, emission, NVH, etc. to keep the problem tractable it is reasonable to focus only the fuel economy in the design of LTV-MPC, while the other considerations can be further handled in practical calibrations.

$$\begin{cases}
0 \leq T_{eng} \leq 180 \text{ N} \cdot \text{m} \\
-260 \text{ N} \cdot \text{m} \leq T_{mot} \leq 260 \text{ N} \cdot \text{m} \\
0.3 \leq SOC \leq 0.7 \\
0 \leq m_f \leq 5,000 \text{ g/s} \\
0 \leq V \leq 40 \text{ m/s}
\end{cases} \tag{13}$$

This optimisation problem can be well solved through quadratic programming, and then the optimal control variable at time k can be obtained and applied to get the optimal torque distribution.

3.2 Transmission ratio optimisation

To optimise the transmission ratio, the torque distribution sequence obtained in the upper LTV-MPC is introduced into the transmission ratio optimisation module as a measurable disturbance. With the input changing to transmission ratio $r_{gear}(i)$, the nonlinear model in equation (6) can be written as follows.

$$\begin{cases}
\dot{x} = f_r(x, u_d, d_r) \\
y = g_r(x, u_d, d_r)
\end{cases} \tag{14}$$

where the state variable and output are the same as that in equation (6), the input $u_d = r_{gear}(i)$, and the disturbance $d_r = [T_{eng}, T_{mot}, F_r]^T$.

Obviously, it is difficult to directly handle the transmission ratio optimisation problem since there exist both discrete and continuous variables. Therefore, convexification processing is adopted to deal with nonlinear equation (14) containing discrete variables. By taking the transmission ratio $r_{gear}(j)$ of each gear j as a constant and introducing corresponding Boolean $\delta_j \in \{0, 1\}$ as input, the convex model can be obtained as follows.

$$\begin{cases} \dot{x}(k+1) = \sum_{j=1}^7 \delta_j f_r(x(k), r_{gear}(j), d_r(k)) \\ y(k+1) = \sum_{j=1}^7 \delta_j g_r(x(k), r_{gear}(j), d_r(k)) \end{cases} \quad (15)$$

According to the state, control input and measurable disturbance at time k , the state and output at each time step within the prediction horizon can be computed iteratively via equation (15). The transmission ratio optimisation problem here can be solved through HMPC, which is similar to that in Pang et al. (2001). With the control input in equation (15) being δ_j , here the corresponding cost function is

$$J_t = \sum_{i=1}^{N_p} \|y(k+i) - y_{ref}(k+i)\|_{Q_t}^2 + \sum_{i=1}^{N_c-1} \|\delta_{k+i}\|_{R_t}^2 \quad (16)$$

where y_{ref} is the same reference output as η_{ref} in equation (11). Q_t and R_t are the weights of output and input, respectively.

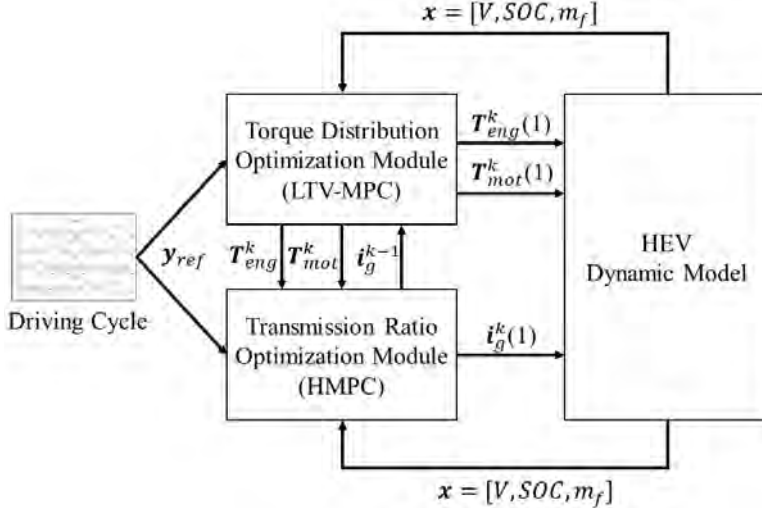
The constraints of gear selection and actuation limits should be considered, as in equation (17). Specifically, when changing gear from m to n at time $k+i$, the speed and torque of engine/motor should be within its maximum and minimum limits. Then, this formulated HMPC problem can be solved via MIQP.

$$\begin{cases} \sum_{j=1}^7 \delta_j = 1 \\ R_w \omega_{eng/mot}^{\min} \leq v_{k+i} i_0 r_{gear}(j) \leq R_w \omega_{eng/mot}^{\max} \\ T_{eng/mot}^{\min} r_{gear}(n) \leq T_{eng/mot}(m) r_{gear}(m) \leq T_{eng/mot}^{\max} r_{gear}(n) \end{cases} \quad (17)$$

The framework of the proposed bi-level controller is schemed in Figure 3, where the upper level optimises the torque distribution and the lower level optimises the transmission ratio. $\mathbf{T}_{eng/mot}^k$ and \mathbf{i}_g^k represent the optimised sequence of engine/motor torque and transmission ratio, respectively, in which \mathbf{i}_g^k contains N_c gear ratio $r_{gear}(i)$, $i = 1, 2, \dots, 7$. At the first optimisation step, the LTV-MPC calculates the optimal engine and motor torque sequence $\mathbf{T}_{eng/mot}^1$ based on the same transmission ratio in the prediction horizon N_p , which is $r_{gear}(1)$. With the optimised engine and motor torque sequence, the lower level optimises corresponding transmission ratio sequence via MIQP. To this end, the first element of the engine and motor torque and transmission ratio sequence is deployed to the bottom controller of the HEV. At each subsequent optimisation step k , the upper level optimises the torque distribution in the prediction horizon based on the

last step's optimised transmission ratio sequence \mathbf{i}_g^{k-1} . Meanwhile, the optimised torque distribution is introduced into the lower level for the optimised transmission ratio sequence \mathbf{i}_g^k at this step k . Then the first element of the torque and transmission ratio sequence, that is $\mathbf{T}_{eng/mot}^k(1)$ and $\mathbf{i}_g^k(1)$, will be deployed so on and on.

Figure 3 The framework of the bi-level controller



4 Simulation

The proposed bi-HMPC controller is first validated through simulations. A proportional-integral-differentiator-based driver model is used to regulate the vehicle speed as close as to the target speed v_{ref} specified in the driving cycle. According to the speed error e , the accelerator/brake pedal opening can be calculated as

$$\alpha = K_P \left(e + K_I \int e dt + K_D \cdot \frac{de}{dt} \right) \quad (18)$$

where α is the accelerator/brake pedal opening, and K_P , K_I and K_D are the proportional, integral and differential gains, respectively.

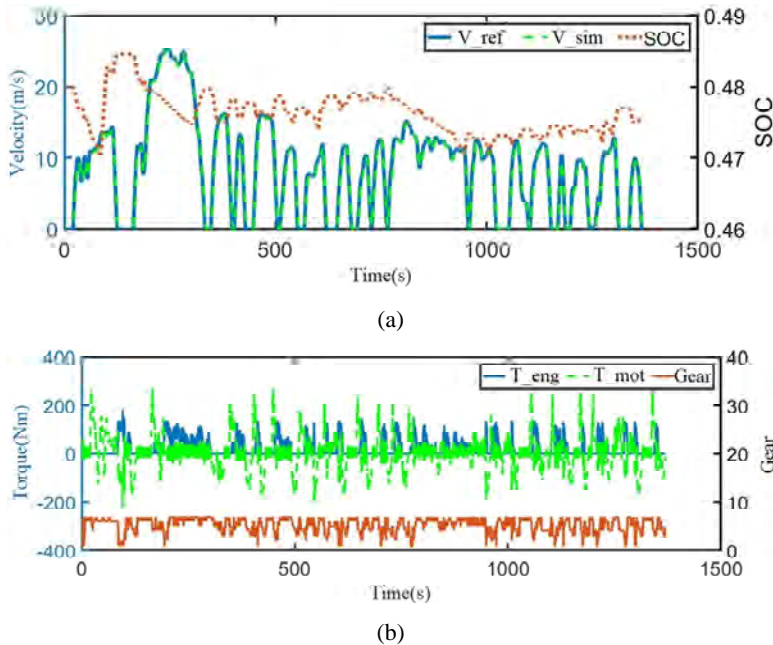
Simulation results in UDDS driving cycle are presented in Figure 4. It shows that the simulated velocity V_{sim} can follow V_{ref} closely, while battery SOC fluctuates slightly around the reference value $SOC_{ref} = 0.48$. On the other hand, it can be found from Figure 4(b) that the vehicle is driven by the motor only when accelerating from rest. Only after the vehicle has started, the engine starts to work and adjusts its operating point via motor torque. By optimising the gear ratio while allowing the engine to operate in a high-efficiency region, the proposed bi-HMPC is able to improve HEV fuel economy to 4.45 L/100 km in UDDS.

Furthermore, the fuel consumption results in various driving cycles are compared in Table 2. With the energy management strategy of ECMS (Pisu and Rizzoni, 2005), the studied HEV's fuel consumption in NEDC, UDDS, LA92 and WLTC are 5.07 L/100 km, 4.62 L/100 km, 5.48 L/100 km and 5.65 L/100 km, respectively. However, when adopting the proposed bi-HMPC, the fuel consumption can be further improved by 5.5%, 3.7%, 12.2% and 7.8%, respectively. As for the computational efficiency of the proposed bi-HMPC, each step in the simulation takes 0.415 s on average when setting $dT = 1$ s, $N_c = N_p = 15$, which is less than half of the sampling time.

Table 3 Simulation results of bi-HMPC and ECMS in different driving cycles ($N_c = N_p = 15$)

Driving cycle	Strategy	L/100 km	Improvement
NEDC	Bi-HMPC	4.79	↓5.5%
	ECMS	5.07	--
LA92	Bi-HMPC	4.81	↓12.2%
	ECMS	5.48	--
UDDS	Bi-HMPC	4.45	↓3.7%
	ECMS	4.62	--
WLTC	Bi-HMPC	5.21	↓7.8%
	ECMS	5.65	--

Figure 4 Bi-level HMPC simulation results (see online version for colours)



It can be drawn from the simulations that the proposed bi-HMPC-based energy management strategy can improve fuel economy of HEV by properly distributing the engine/motor torque and optimising the gear ratio. With the rapid development of the

computing performance of on-board controllers, the proposed bi-HMPC has the potential of real-vehicle application to further improve fuel economy of HEVs.

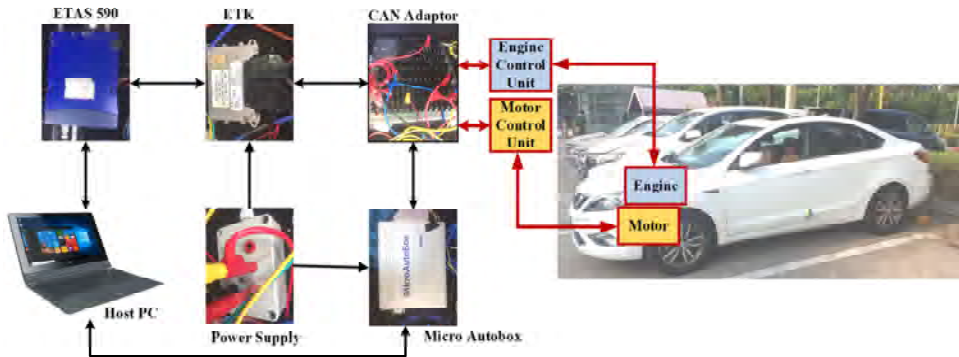
5 Real vehicle validation of LTV-MPC

To further validate the practical performance of bi-HMPC, we implement the proposed LTV-MPC algorithm in this P2 structure HEV. However, since the transmission of the studied HEV is provided by another supplier and can only be controlled separately by its own controller, it is challenging to implement both optimisation of torque distribution and transmission ratio in this vehicle. Therefore, here only the upper level LTV-MPC-based torque optimisation module is validated in the real vehicle.

The real-time test of algorithm implementation is schemed in Figure 5, which includes ETK, ETAS 590, adaptor, dSPACE MicroAutoBox, host PC, and 12 V power supply. Among them, MicroAutoBox is used for the real-time calculation of LTV-MPC algorithm; ETK is the prototype vehicle controller; ETAS 950 can modify the control parameters of the vehicle controller through the host PC; and adaptor facilitates debugging via CAN ports. ETAS bypasses the original algorithm in ETK, so that ETK only receives the control command calculated in MicroAutoBox, which runs the LTV-MPC algorithm based on feedback vehicle information via adaptor. A chassis dynamometer based on the NEDC driving cycle is adopted.

The vehicle is first tested in passive mode, with the final fuel consumption result as 5.4 L/100 km (NEDC). Note that the original hybrid energy management algorithm is developed via RB, and the development team has taken several months or even years of work, including more than ten rounds of bench tests, before arriving this performance. In this research, one main objective is to show whether the model-based LTV-MPC approach can help accelerate the HEV algorithm development process.

Figure 5 Schematic diagram of algorithm tests (see online version for colours)



5.1 Preliminary test

To check whether the top-down design process works or not, we run the preliminary test without any adjustment. Fuel consumption and emission results are shown in Table 4, where the corresponding mass of emissions include carbon dioxide CO_2 , carbon monoxide CO , hydrocarbon HC , non-methane hydrocarbon NMHC and nitrogen oxides

NO_x. The vehicle fuel consumption reaches 7.03 L/100 km and CO₂ emissions is up to 163.48 g/km. Compared to the original powertrain performances, both the fuel economy and emission are far from acceptable, indicating that the empirical setting of MPC in Subsection 3.1 is not satisfactory.

Figure 6 presents the engine and motor torques during the test, including the required torques by LTV-MPC ($T_{motor/eng}^{require}$) and the realised torques by the engine or motor controllers ($T_{motor/eng}^{actual}$). It shows that for both engine and motor, there are certain differences between the required and the actual torque, indicating that the corresponding controllers, especially the engine controller, cannot respond well the fast torque demand. Meanwhile, the engine torque varies too much and its maximum torque exceeds 150 Nm. Figure 7 further shows that the engine starts and stops frequently (17 times) under the whole cycle conditions. To summarise, it can be speculated that the main reasons for high fuel consumption include:

- 1 frequent start and stop of the engine
- 2 the engine torque fluctuates up and down
- 3 the peak of engine torque is too high.

Figure 6 Engine/motor torques in preliminary bench testing (see online version for colours)

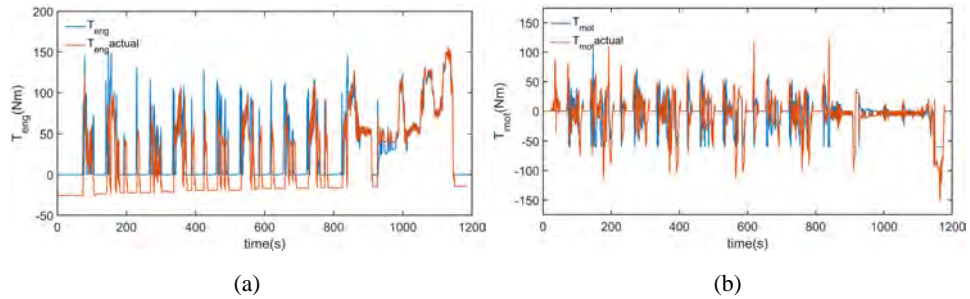
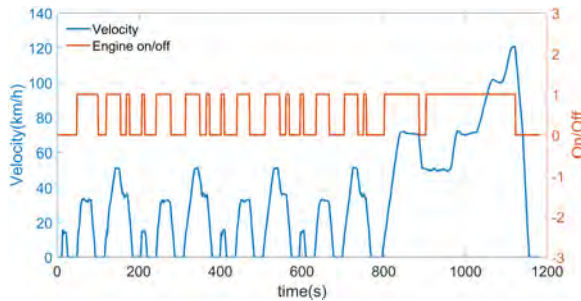


Figure 7 Engine start-stop in preliminary bench testing (see online version for colours)



5.2 Algorithm improvements

Based on above speculation, for improvements we set the engine to keep off when vehicle speed is lower than 16 km/h and the engine needs to be kept on for at least 30 s after starting, which is implemented outside the LTV-MPC with a rule-based controller.

Besides, in the LTV-MPC cost function (11), the weight of the engine torque increment is increased to ensure the torque changes more smoothly.

The improved algorithm is further examined in a 2nd-round drum test, with results shown in Table 4. The vehicle fuel consumption was 6.41 L/100 km, which has already been 8.8% smaller than that in the preliminary test. However, the pollutant emissions seem deteriorated to a certain extent except for CO₂.

Through the comparison and analysis of the two results through Figures 8 and 9, it can be seen that after the control parameters modification, the engine has fewer start-stops and smaller torque fluctuations, which greatly improves the fuel economy. However, there is still a problem of excessive torque when the engine is being activated ON.

Figure 8 Comparison of engine torque in two tests (see online version for colours)

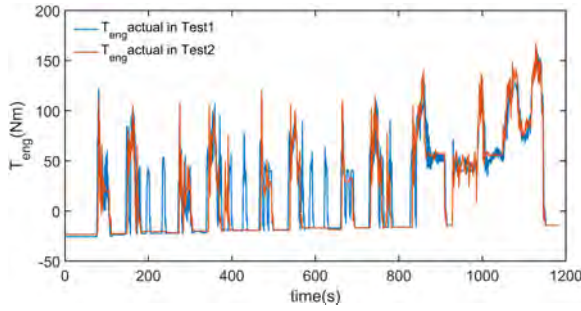
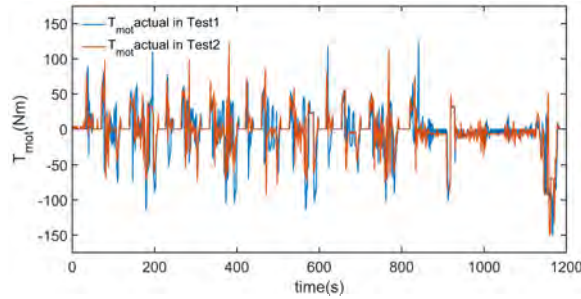


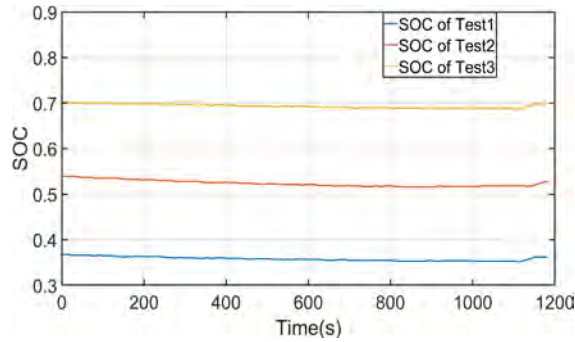
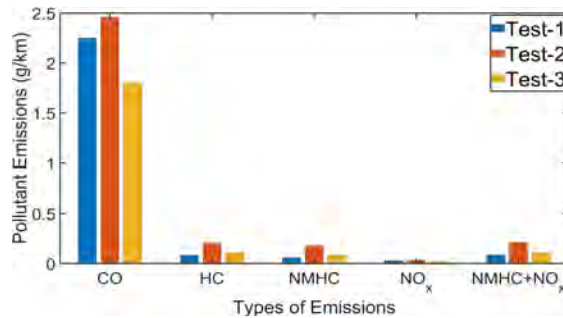
Figure 9 Comparison of motor torque in two tests (see online version for colours)



To limit the initial engine torque when it is switched ON, we further restrict the engine starting torque via the rule-based controller. In addition, the weight of the engine torque increment in the cost function (11) is further increased to restrict the fluctuation of engine torque. For the LTV-MPC controller, the prediction, control horizon and discretisation step are set to $N_p = 20$, $N_c = 10$ and $dT = 0.2$ s, respectively. Then the 3rd-round test results are shown in Table 4. The vehicle fuel consumption is now 6.20 L/100 km, which is a reduction of 3.3% compared to the 2nd-round test. CO₂ emission is reduced to 144.49 g/km, and NO_x is also reduced to 0.018 g/km. To justify the comparability of these three tests, Figure 10 presents the corresponding battery SOC curves. Though the initial SOC of three experiments are different, the SOC changes Δ SOC are very small (0.007, 0.012, and 0.005, respectively).

Table 4 The overall bench testing results under NEDC driving cycle

Test round	Fuel consumption (L/100 km)	CO ₂ (g/km)	CO (g/km)	HC (g/km)	NMHC (g/km)	NO _x (g/km)	NMHC + NO _x (g/km)
1st	7.03	163.48	2.248	0.083	0.059	0.029	0.088
2nd	6.41	148.15	2.456	0.203	0.177	0.034	0.211
3rd	6.20	144.49	1.797	0.109	0.089	0.018	0.106

Figure 10 Battery SOC in three tests (see online version for colours)**Figure 11** Comparison of emissions in three experiments (see online version for colours)

By applying LTV-MPC algorithm, the vehicle fuel consumption has been reduced to 6.2 L/100 km after only three round adjustments. Moreover, reduction of main emissions can also be seen from the comparison in Figure 11. With the linearised system model of energy management problem, the objective function can be well solved via quadratic programming while meeting various constraints, e.g., actuator limit, state variable boundary. Comparing with the original nonlinear MPC formulation, the LTV-MPC can significantly reduce computational burden and is possible for real implementation. Note that this is achieved with no direct control over transmission shifting strategy, that is, the lower level of transmission optimisation is not applied in real vehicle experiment. It is possible to achieve better results of fuel economy if the shifting can also be optimised and controlled. The efficient process of performance improvements by combining the expert rules shows that the optimisation framework of LTV-MPC can guarantee straightforward and effective development of HEV energy management algorithm.

6 Conclusions

We propose a bi-HMPC-based energy management algorithm for a P2 HEV, whose upper level distributes the optimal engine/motor torque via LTV-MPC and lower level optimises the gear ratio based on HMPC. Simulation results validate that the proposed bi-HMPC improves HEV's fuel consumption over ECMS by 5.5%, 3.7%, 12.2% and 7.8% under NEDC, UDDS, LA92 and WLTC driving cycles, respectively. The further validation of the upper LTV-MPC is carried out in the real vehicle experiments, showing that this framework is effective in handling fuel economy improvements, with fuel consumption reduced from 7.05 L/100 km to 6.2 L/100 km within only three drum tests. With the improvement of computing efficiency, the LTV-MPC algorithm has the potential for real-vehicle applications.

In this research, one main objective is to show how the model-based approach can help accelerate the HEV algorithm development process. The hybrid energy management algorithm in the original vehicle is developed via RB, which have taken several months or even years of work before arriving the final fuel consumption result of 5.4 L/100 km (NEDC). However, with only three rounds of tuning, the model-based LTV-MPC can reduce the fuel consumption from 7.03 L, to 6.41 L and finally to 6.2 L/100 km, showing it has a great potential to accelerate the hybrid vehicle algorithm development. This framework can be also flexibly combined with expert rules for further considerations of emission and NVH, etc.

Note that due to limits of funding the precise modelling of engine, motor, battery and transmission is unfortunately impossible at the current stage of research. Considering the system complexities of hybrid powertrain and vehicle, to keep the problem still tractable we can only focus on fuel economy in the optimisation. For OEM implementations, the detailed modelling and even the lower-level control (e.g., transmission gear ratio) are all possible, in which case more promising performances of the LTV-MPC framework can be expected.

Acknowledgements

This work was supported by the Department of Science and Technology of Zhejiang under Grant 2022C01241 and 2023C01238. The experimental works are supported by the Engineering Innovation and Training Center in Polytechnic Institute of Zhejiang University.

References

- Bayindir, K.Ç., Gözükcük, M.A. and Teke, A. (2011) 'A comprehensive overview of hybrid electric vehicle: powertrain configurations, powertrain control techniques and electronic control units', *Energy Convers. Manag.*, Vol. 52, No. 2, pp.1305–1313.
- Borhan, H., Vahidi, A., Phillips, A.M., Kuang, M.L., Kolmanovsky, I.V. and Di Cairano, S. (2011) 'MPC-based energy management of a power-split hybrid electric vehicle', *IEEE Trans. Control Syst. Technol.*, Vol. 20, No. 3, pp.593–603.

- Borhan, H.A., Zhang, C., Vahidi, A., Phillips, A.M., Kuang, M.L. and Di Cairano, S. (2010) 'Nonlinear model predictive control for power-split hybrid electric vehicles', in *49th IEEE Conference on Decision and Control (CDC)*, December, pp.4890–4895, DOI: 10.1109/CDC.2010.5718075.
- Cairano, S.D., Bemporad, A., Kolmanovsky, I.V. and Hrovat, D. (2007) 'Model predictive control of magnetically actuated mass spring dampers for automotive applications', *Int. J. Control*, Vol. 80, No. 11, pp.1701–1716.
- Iyama, H. and Namerikawa, T. (2014) 'Fuel consumption optimization for a power-split HEV via gain-scheduled model predictive control', in *2014 Proceedings of the SICE Annual Conference (SICE)*, pp.468–473.
- Jiang, D., Li, D. and Yu, X. (2020a) 'Energy management of HEV based on hybrid model predictive control', *Journal of Jilin University (Engineering and Technology Edition)*, Vol. 50, No. 4, pp.1217–12261.
- Jiang, D., Li, D. and Yu, X. (2020b) 'Model predictive control energy management based on driver demand torque prediction', *Journal of Zhejiang University (Engineering Science)*, Vol. 54, No. 7, pp.1325–1334+1361.
- Lee, J.H. (2011) 'Model predictive control: review of the three decades of development', *Int. J. Control Autom. Syst.*, Vol. 9, No. 3, pp.415–424.
- Lin, C.-C., Peng, H. and Grizzle, J.W. (2004) 'A stochastic control strategy for hybrid electric vehicles', in *Proceedings of the 2004 American Control Conference*, Vol. 5, pp.4710–4715.
- Liu, J. and Peng, H. (2008) 'Modeling and control of a power-split hybrid vehicle', *IEEE Trans. Control Syst. Technol.*, Vol. 16, No. 6, pp.1242–1251.
- Mordor Intelligence (2021) *Hybrid Vehicle Market – Growth, Trends, and Forecast (2021–2026)* [online] <https://www.mordorintelligence.com/industry-reports/hybrid-vehicle-market> (accessed 7 August 2021).
- Musardo, C., Rizzoni, G., Guezennec, Y. and Staccia, B. (2005) 'A-ECMS: an adaptive algorithm for hybrid electric vehicle energy management', *Eur. J. Control*, Vol. 11, Nos. 4–5, pp.509–524.
- Pang, S., Farrell, J., Du, J. and Barth, M. (2001) 'Battery state-of-charge estimation', in *Proceedings of the 2001 American Control Conference*, Vol. 2, Cat. No. 01CH37148, pp.1644–1649.
- Pisu, P. and Rizzoni, G. (2005) 'A supervisory control strategy for series hybrid electric vehicles with two energy storage systems', in *2005 IEEE Vehicle Power and Propulsion Conference*, 8pp.
- Pisu, P., Koprubasi, K. and Rizzoni, G. (2005) 'Energy management and drivability control problems for hybrid electric vehicles', in *Proceedings of the 44th IEEE Conference on Decision and Control*, pp.1824–1830.
- Serrao, L., Onori, S. and Rizzoni, G. (2009) 'ECMS as a realization of Pontryagin's minimum principle for HEV control', in *2009 American Control Conference*, pp.3964–3969.